

Received September 2, 2019, accepted September 19, 2019, date of publication September 25, 2019, date of current version October 10, 2019.

Digital Object Identifier 10.1109/ACCESS.2019.2943611

# Dual-Polarized Communication Rectenna Array for Simultaneous Wireless Information and Power Transmission

GE-LIANG ZHU<sup>1</sup>, JIN-XIN DU<sup>1</sup>, XUE-XIA YANG<sup>2</sup>, (Senior Member, IEEE),  
YONG-GANG ZHOU<sup>3</sup>, (Member, IEEE), AND STEVEN GAO<sup>4</sup>, (Fellow, IEEE)

<sup>1</sup>School of Communication and Information Engineering, Shanghai University, Shanghai 200072, China

<sup>2</sup>Key Laboratory of Specialty Fiber Optics and Optical Access Networks, Shanghai Institute for Advanced Communication and Data Science, Shanghai University, Shanghai 200444, China

<sup>3</sup>College of Electronic and Information Engineering, Nanjing University of Aeronautics and Astronautics, Nanjing 211106, China

<sup>4</sup>School of Engineering and Digital Arts, University of Kent, Canterbury CT2 7NZ, U.K.

Corresponding author: Xue-Xia Yang (yang.xx@shu.edu.cn)

This work was supported by the National Natural Science Foundations of China under Grant 61771300.

**ABSTRACT** A dual-polarized communication rectenna array with high isolation and low cross polarization for simultaneous wireless information and power transmission (SWIPT) is presented. It consists of a  $2 \times 2$  element receiving antenna array and a high efficiency rectifier based on voltage doubler topology. The receiving element is corner-fed to achieve high isolation of more than 20 dB between the dual-polarized ports, which guarantees low mutual interference between the communication and the rectifying ports. To receive enough electromagnetic (EM) wave for rectifying and meanwhile meet the communication sensitivity, this  $2 \times 2$  array uses its  $2 \times 2$  vertical polarization ports and  $1 \times 2$  horizontal polarization ports for power rectifying, and the rest  $1 \times 2$  horizontal polarization ports for communication. For the communication port, the measured gain is 10.9 dBi and the cross polarization is less than  $-20$  dB. The performance of the whole communication rectenna array has been measured, where a  $2 \times 4$  circularly-polarized array with a gain of 17.5 dBi, settled 1 meter away is used as the transmitter. Measured results show that the system achieves a peak microwave – direct circuit (mw-dc) conversion efficiency of 74.9 % for the CW signal, and 67 % for the QPSK signal with 10 MHz channel bandwidth on the load of  $345 \Omega$  at 2.58 GHz operating frequency.

**INDEX TERMS** Simultaneous wireless information and power transmission (SWIPT), rectenna array, rectifier, conversion efficiency.

## I. INTRODUCTION

With the pervasive expansion of the wireless technology in people's daily life, the requirement for wireless devices has experienced rapid growth in recent years [1]. However, the limited battery capacity remains a bottleneck that restricts the durability and portability of wireless devices [2]. There is an urgent need to address the problem of efficiently powering wireless devices before their massive deployment for thriving applications such as 5G, Internet of Things (IoT) [3], [4], Wireless Sensor Networks (WSN) [5], etc. Today, electronic devices like mobile phones and medical implants can be charged by the way of electromagnetic induction, and the

highest power transfer efficiency could be over 90 %. However, the distance between transmitter and receiver is limited to the order of millimeter or centimeter [6]. Microwave Power Transmission (MPT) technology, which used to supply high power to helicopters and high-altitude aircrafts [7]–[10], could be a promising method to overcome this difficulty. MPT enables remote replenishment of electric power to wireless devices in a long distance and avoids frequent replacement of battery, which makes wireless devices become more portable, self-sustainable, and longevity.

Generally, when the receiver of a wireless communication system extracts information contained in the received EM wave, the EM power is wasted. If the receiver could effectively collect the EM energy and supply it to the terminal devices while exchanging information, the performance of

The associate editor coordinating the review of this manuscript and approving it for publication was Andrei Muller<sup>1</sup>.

the whole communication system will be improved greatly in several aspects, such as spectral efficiency, lower network operation cost, and particularly, lower power consumption [1]. In 2008, Varshney et al. proposed the Simultaneous Wireless Information and Power Transfer (SWIPT) [11], which implies the information and power transmission at the same time. Followed that, some researchers analyzed the relationship between the channel rate, channel capacity and energy efficiency in SWIPT [12]–[15]. The MIMO (Multiple-Input Multiple-Output) system has been suggested to realize SWIPT in [16], where how the energy supplied to the receiver affects the optimal communication strategy has been studied.

A rectenna, consisting of a receiving antenna and a rectifying circuit, can receive EM wave power and convert it into dc power. The microwave-direct current (mw-dc) conversion efficiency could be about 75 % when the frequency is below 10 GHz [17]–[19]. A linear-polarized rectenna for SWIPT usage was proposed in [19], where transmitting EM wave power and information alternated at the different time. A dual-polarized rectenna with data communication capability was proposed in [20], where the two orthogonal polarization ports were used as transferring power and information simultaneously. The measured mw-dc conversion efficiency is 64 % at 5.8 GHz operating frequency and the communication performance was not evaluated.

In this paper, we propose a novel  $2 \times 2$  communication rectenna array for SWIPT. The antenna element is an aperture-coupled corner-fed dual-polarized patch antenna, which has high isolation and low cross polarization between each port. The  $2 \times 1$  horizontal polarization ports and the  $2 \times 2$  vertical polarization ports of the communication rectenna array are used for power rectifying, while the rest  $1 \times 2$  horizontal polarization ports are used for communication. The feeding network is designed to appropriately allocate the received signal to rectification and communication, ensuring the high performance of the entire SWIPT system.

The rest of the paper is organized as follows. Section II introduces the whole SWIPT system. Section III introduces the design of the receiving antenna with high isolation. Section IV presents the design and measurements of the high efficiency rectifier. The rectifying efficiency for CW, 64QAM and QPSK signals are measured. In Section V, the design of the entire communication rectenna array is illustrated, the information transmission test is carried out, and the conversion efficiency for QPSK and CW signals are also measured. Finally, conclusion is drawn in Section VI.

## II. THE SWIPT SYSTEM

The SWIPT system consists of two parts: the transmitter that transmits the CW or modulated signals at required power level; and the receiver that receives the EM waves, some of which are converted into dc power and another part for the information extraction at the same time. Fig. 1 illustrates the SWIPT system, which operates at 2.6 GHz central frequency. In the transmitter, the CW or modulated signals are generated by a signal generator, then amplified by a solid-state

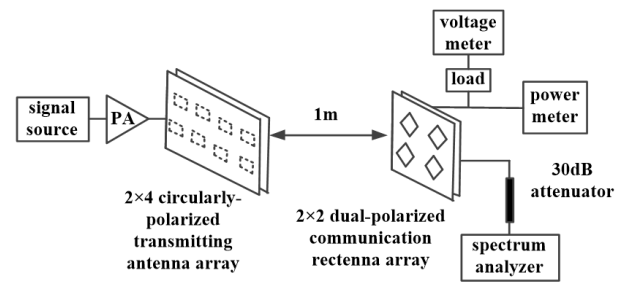


FIGURE 1. Schematic of the SWIPT system.

power amplifier. The EM signal is transmitted by a high gain  $2 \times 4$  element circular-polarized antenna array, and all the EM energy would be received by the dual-polarized antenna.

The dual-polarized communication rectenna array is fixed at 1 meter distance away from the transmitting antenna array, which is in the near-field region. It should be informed that this distance could be extended if the transmitting power is high or the receiver has high sensitivity. The communication ability of the rectenna array will be verified by analyzing the output signal from the communication port with the help of a spectrum analyzer. An attenuator is used to reduce the signal amplitude and protect the spectrum analyzer. The EM power received by the array will be measured by the power meter. The output dc voltage across the load will be measured using a voltage meter, from which the output dc power can be calculated.

## III. RECEIVING ANTENNA WITH HIGH ISOLATION

The interference between the power channel and the information channel must be minimized in order to reach high SWIPT performance. This could be achieved by adopting a dual-polarized antenna with high isolation, so that the power and information can be transmitted in different polarization ports at the same time. Moreover, compared with the traditional side-feeding [20], the corner-feeding provides high isolation of 30 dB between different ports and reduces the cross polarization [21].

We propose an aperture-coupled corner-fed dual-polarized patch antenna, as shown in Fig. 2. The antenna has three substrate layers and one air layer. The square radiation patch is etched on the top of layer 2, and a square parasitic patch is on the top of layer 1. These two layers are separated by an air layer. Two orthogonal H-shape apertures are etched on the ground, which is on the top of layer 3. Two microstrip feeding lines are on the bottom of layer 3. The operating frequency is mainly determined by the side length of the square radiation patch. The introduction of the parasitic patch could broaden the impedance bandwidth and enhance the gain. The rectifier will be placed on the feeding layer, so that the influence of the rectifier on the antenna can be reduced greatly. This multi-layer structure is also beneficial for obtaining higher gain and broader bandwidth.

The substrate is F-4B with the relative dielectric constant  $\epsilon_r = 2.65$  and loss tangent  $\tan\delta = 0.001$ . The antenna was simulated using the HFSS software. The geometrical

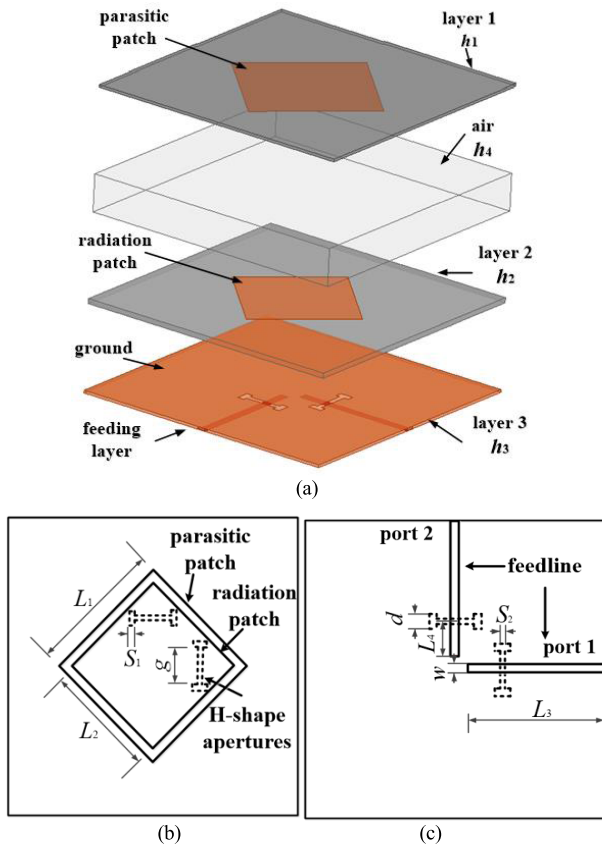


FIGURE 2. Configuration of the dual-polarized antenna: (a) perspective view, (b) top view, (c) bottom view.

parameters are  $h_1 = h_3 = 0.8$  mm,  $h_2 = 1.5$  mm,  $h_4 = 11$  mm,  $L_1 = 36$  mm,  $L_2 = 31.5$  mm,  $L_3 = 36.5$  mm,  $L_4 = 9.5$  mm,  $S_1 = 2$  mm,  $S_2 = 1.5$  mm,  $g = 10$  mm,  $d = 4$  mm,  $w = 2.37$  mm.

The antenna was measured using the Vector Network Analyzer (VNA) Agilent 8722ES. The simulated and measured S parameters are plotted in Fig. 3. The simulated  $-10$  dB bandwidth of the reflection coefficients  $|S_{11}|$  and  $|S_{22}|$  are both 426 MHz (16.4 %), while the measured results are 410 MHz (15.8 %) and 400 MHz (15.4 %), respectively. The measured lowest value of  $|S_{11}|$  and  $|S_{22}|$  are  $-20$  dB and  $-25$  dB at their corresponding center frequencies. The measured results show that the antenna is well matched in a wideband region. The measured isolation  $|S_{21}|$  between two ports is higher than 20 dB within a broad bandwidth, implying very low interference between two ports. Fig. 4 shows the simulated and measured radiation patterns of each port. The maximum gain was observed to be as high as 8.2 dBi in simulation and 8 dBi in measurement at the central frequency of 2.6 GHz for each port. The cross polarization is  $-23$  dB in simulation and  $-20$  dB in measurement. The measured front-to-back ratio is more than 15 dB.

IV. THE RECTIFIER DESIGN AND MEASUREMENTS

A. DESIGN OF THE RECTIFIER

The voltage doubler topology is adopted for the rectifier design, which is more favorable in case of high input power.

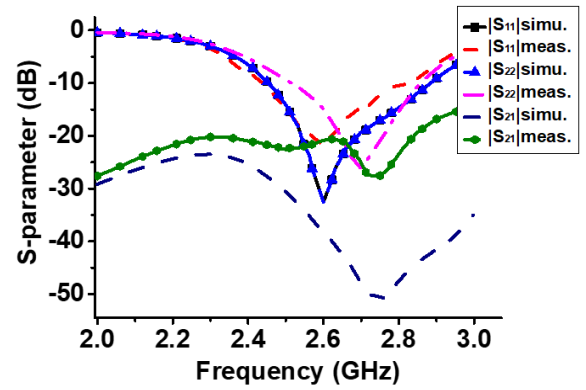


FIGURE 3. S-parameters of the antenna versus frequency.

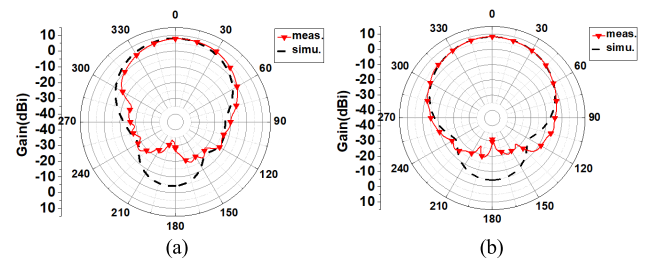


FIGURE 4. Simulated and measured radiation patterns of two ports: (a) Port 1, (b) Port 2.

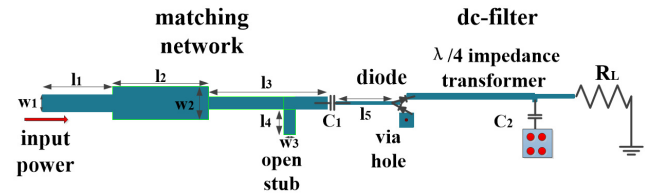


FIGURE 5. Schematic of the rectifier.

The rectifier consists of an impedance matching network, a rectifying diode, a dc-pass filter and a load, as shown in Fig.5. The open stub is introduced to cancel out the imaginary part of the diode’s input impedance. Multi-step microstrip line expands the bandwidth. The dc-pass filter contains a  $\lambda/4$  impedance transformer and a capacitor, which suppresses the high order harmonics and smooth the output dc voltage. The dimensions are  $l_1 = 9.4$  mm,  $l_2 = 12.4$  mm,  $l_3 = 12.9$  mm,  $l_4 = 3.2$  mm,  $l_5 = 7.5$  mm,  $w_1 = 2.2$  mm,  $w_2 = 3.5$  mm,  $w_3 = 1.5$  mm,  $C_1 = C_2 = 47$  pF.

The adopted diode is a packaged Schottky diode HSMS2822. It has high reverse breakdown voltage and low power loss, which is favorable for high power rectifying. The equivalent parameters of the diode are: built-in turn-on voltage  $V_{bi} = 0.34$  V, series resistance  $R_s = 6 \Omega$ , zero-biased junction capacitance  $C_{j0} = 0.7$  pF, and reverse breakdown voltage  $V_{br} = 15$  V. As the input power increases, the junction capacitance of the diode decreases, thereby improving the rectifying efficiency [22]. The simulation using ADS

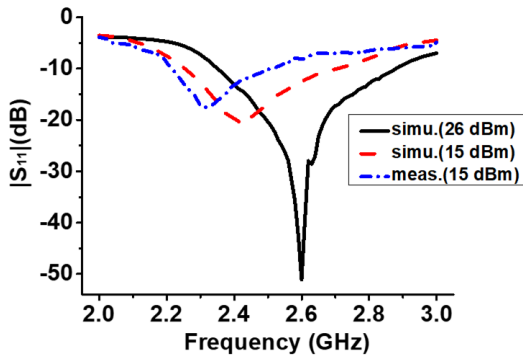


FIGURE 6. Reflection coefficient of the rectifier.

software shows that, the input impedance of the diode at 2.6 GHz is  $(57 - j31) \Omega$  when the input power is 26 dBm and the load is  $421 \Omega$ . The substrate is the same as that for the receiving antenna and the thickness is also 0.8 mm.

Simulated and measured  $|S_{11}|$  versus operating frequency is shown in Fig. 6. At the optimal input power of 26 dBm, the simulated  $|S_{11}|$  is less than  $-10$  dB from 2.34 to 2.89 GHz (21.5 %). Because the maximum output power of the VNA is limited to 15 dBm, we measured the  $|S_{11}|$  with an input power of 15 dBm and compared to the simulated one. The measured  $-10$  dB band is from 2.21 to 2.52 GHz (12 %), which remains wide but exhibits some deviation towards the lower frequency. This could be due to the introduction of the parasitic parameters during the fabrication, which decreases the resonant frequency of the rectifier.

**B. RECTIFYING EFFICIENCY FOR CW SIGNAL**

The rectifier measurement system is illustrated in Fig. 7. The rectifying efficiency for the CW signal was measured firstly. The CW signal was generated by the signal source R&S-SMW200A, and then amplified by the solid-state amplifier AV38701C. The amplified microwave power was then injected into the rectifier. A directional coupler was added between the amplifier and the rectifier in order to sample the input power, then send it into a power meter (Agilent E4416A) for monitoring. An attenuator was used for the purpose of protecting the power meter. The output voltage across the load was measured with a voltage meter. The rectifying efficiency can be calculated using the following formula:

$$\eta = \frac{P_0}{P_{in}} = \frac{V_0^2}{P_{in}R_L} \tag{1}$$

where  $P_0$  is the output dc power,  $P_{in}$  is the input power,  $V_0$  is the output dc voltage, and  $R_L$  is the ohmic load.

Fig. 8 shows the simulated and measured rectifying efficiency versus operating frequency, input power and load. From Fig. 8(a), the rectifying efficiency keeps more than 75 % and remains stable within the frequency ranging from 2.57 to 2.62 GHz. The maximum efficiency of 78.7 % is measured at 2.59 GHz frequency, which is a slight decrease

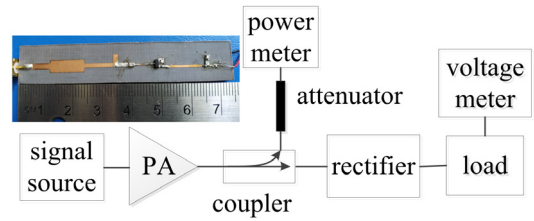


FIGURE 7. The rectifier measurement system.

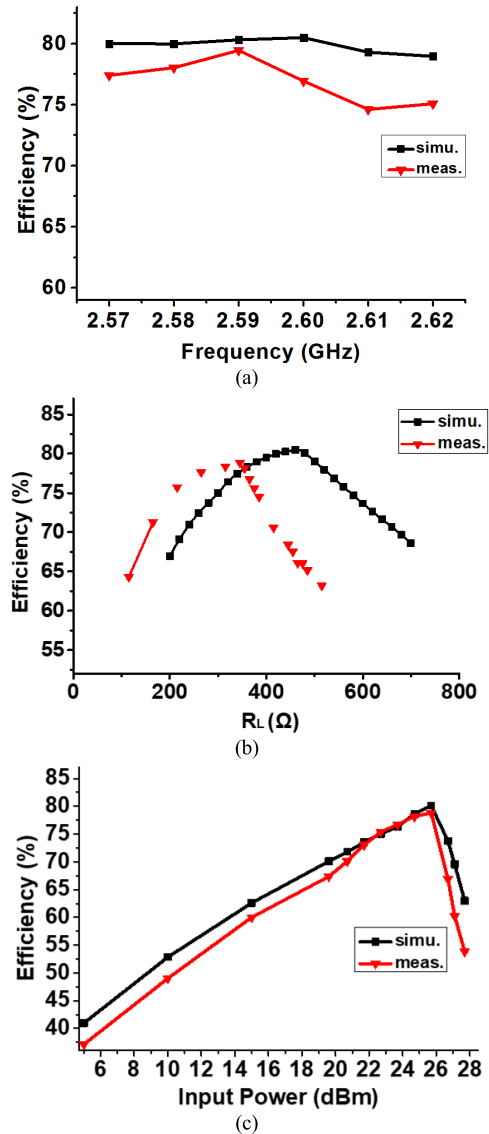
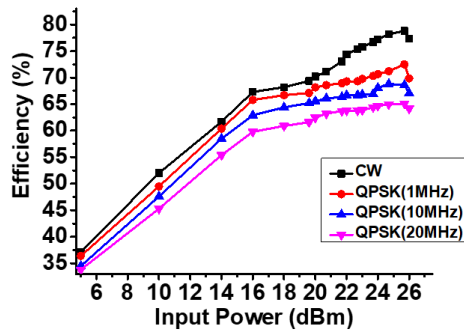
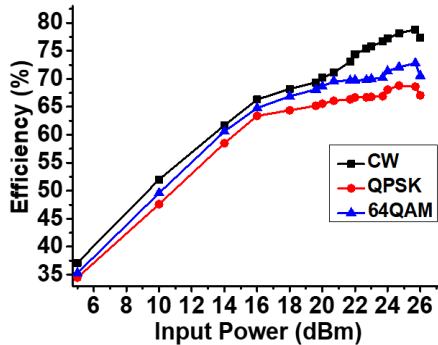


FIGURE 8. Measured and simulated efficiency of the rectifier for CW signal versus: (a) operating frequency, (b) load, (c) input power.

of 1.8 % compared with the simulated one of 80.5 %. Fig. 8(b) shows the rectifying efficiency on different loads with the fixed input power of 25.6 dBm at 2.59 GHz. The highest efficiency of 78.7 % is obtained when the load is  $345 \Omega$ , and the efficiency is over 70 % on the load range from 155 to  $415 \Omega$ . However, there is a deviation between the simulation and measurement. Fig. 8(c) shows that the measured optimal



(a)



(b)

FIGURE 9. Measured efficiency of the rectifier for modulated signals: (a) QPSK signal with different bandwidth, (b) different modulated signals.

input power for the rectifier is 25.6 dBm, which agrees well with the simulation. The efficiency at 20.6 to 26.4 dBm is over 70 % within the power range from 20.6 to 26.4 dBm, which means the rectifier could adapt to different power levels. The little differences between the simulated and the measured results are probably due to the inaccurate fabrication and the equivalent circuit parameters of the diode.

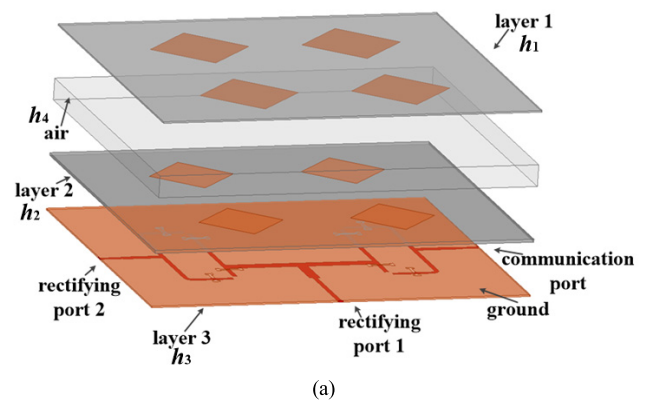
C. RECTIFYING EFFICIENCY FOR MODULATED SIGNAL

The measurement system for the modulated signals is the same as the one in Fig. 7, except that the signal source is of type Agilent E4438C. When the input signals are QPSK signals, the efficiency for different signal bandwidth is shown in Fig. 9(a). The rectifying efficiency for QPSK signals is lower than that for the CW signal. In addition, the efficiency for QPSK signals decreases when the bandwidth increases. When the input power is 25.6 dBm and the bandwidth is 1,10, and 20 MHz the rectifying efficiency is 72.4 %, 68.6 %, and 65.1 %, respectively. Fig. 9(b) illustrates the rectifying efficiency for CW, 64QAM and QPSK signals. The bandwidth of 64QAM and QPSK signal are both 10 MHz. It is noted that the CW signal has the highest efficiency, then the 64QAM signal, and the QPSK signal has the least efficient.

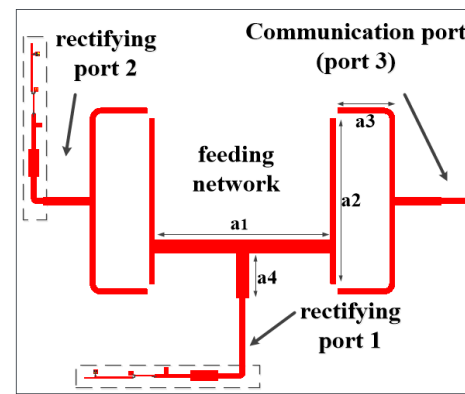
V. THE COMMUNICATION RECTENNA ARRAY

A. DESIGN OF THE COMMUNICATION RECTENNA ARRAY

In order to achieve more adequate receiving power during the SWIPT process, we propose a 2x2 communication rectenna



(a)



(b)

FIGURE 10. Configuration of the array: (a) perspective view of receiving antenna array, (b) bottom view of communication rectenna array.

array. The array is designed in a dual-polarization based on the element proposed in Section III, so the EM wave power and information transmission could operate in different polarization ports with high isolation. The structure of the communication rectenna array is displayed in Fig. 10(a). Information transmission and power rectifying have different requirements on the minimum power level. For example, a typical information receiver can operate with a sensitivity of -60 dBm received signal power, while an energy receiver needs up to -10 dBm signal power [2]. Therefore, most of the received EM signals should be used for power rectifying, and a small part for the information communication.

The feeding network of the communication rectenna array is shown in Fig. 10(b). Among the 4 horizontal ports and 4 vertical ports of the array, the 2x2 vertical ports and 2x1 horizontal ports, denoted as the rectifying port 1 and 2, are used to rectify EM wave power; the 1x2 horizontal port, denoted as the communication port or port 3, are used to transmit information. This novel structure allocates more EM wave power for rectifying, which improves the power-utilization. The power dividing network compensates the phase difference between the upper patch and lower patch of the rectifying port 2 or the communication port through the  $\lambda_g/2$  microstrip line.  $\lambda_g$  is the waveguide wavelength. The input impedance is matched through  $\lambda_g/4$  microstrip impedance converter. The rectifiers are printed on the back

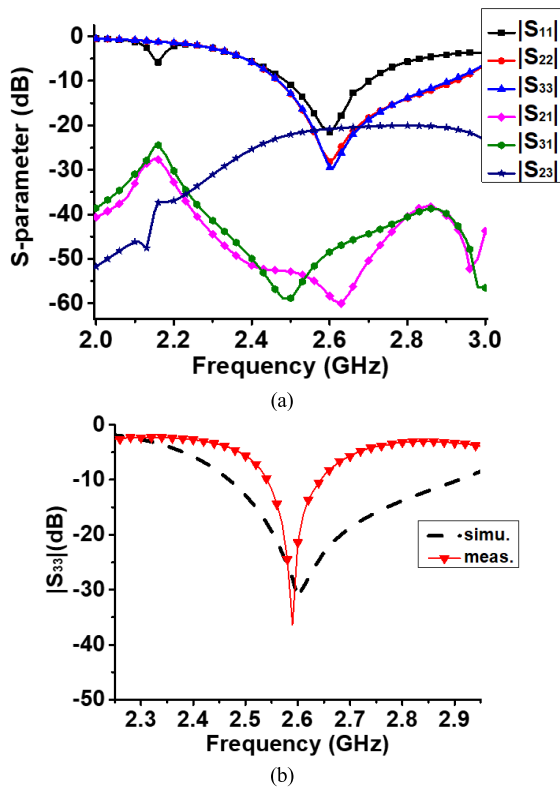


**FIGURE 11.** Simulation and measurement of the S parameters: (a) simulated S parameters of receiving antenna array, (b) measured  $|S_{33}|$  for communication port of communication rectenna array.

of the array and connected to the ports 1 and 2 of the antenna array. The dimensions are  $a_1 = 77.6$  mm,  $a_2 = 73$  mm,  $a_3 = 25.2$  mm,  $a_4 = 20$  mm. The thickness of each layer is the same as the ones of the receiving antenna element. The space between each antenna element is 80 mm ( $0.69 \lambda_0$ ).

### B. SIMULATION AND MEASUREMENT OF THE ANTENNA ARRAY

The simulated S parameters of the receiving antenna array (without rectifiers) are shown in Fig. 11(a). The  $-10$  dB impedance bandwidth is 220 MHz (8.5 %), 460 MHz (17.7 %) and 420 MHz (16.2 %) for the rectifying port 1, 2 and 3, respectively. The reflection coefficients are less than  $-20$  dB at the center frequencies, implying good impedance matching for all ports. The isolation between each port is greater than 20 dB, so that the information and power transmission can be done with almost no interference.

The reflection coefficient  $|S_{33}|$  of the communication port of the fabricated communication rectenna array is measured and illustrated in Fig. 11(b). The  $-10$  dB impedance bandwidth is 150 MHz (5.8 %), which exhibits some reduction compared to the simulation result of  $|S_{33}|$  in Fig. 11(a). The reason probably lies in the integration of the rectifiers on the other two ports, which has an impact on the impedance adaptation of the communication port.

Fig. 12 shows the simulated gain of the array versus frequency when port 1, 2 are separately excited, the maximum

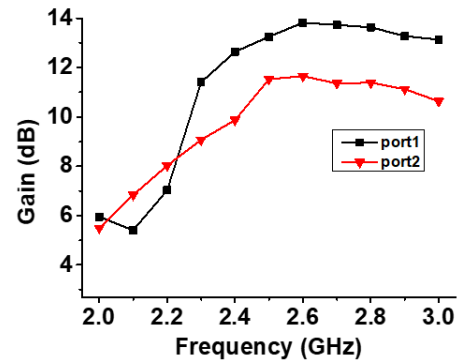


**FIGURE 12.** Simulated antenna gains versus frequency of ports 1 and 2.

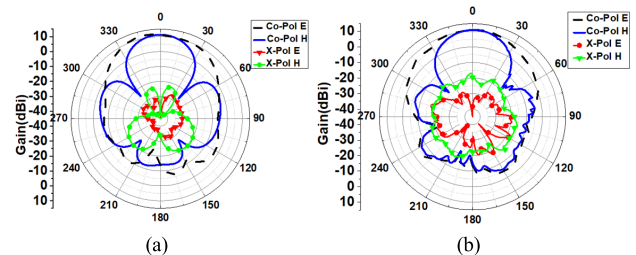


**FIGURE 13.** Patterns of the communication port: (a) simulation, (b) measurement.

gain at the center frequency is 13.8 and 11.2 dBi, respectively. The simulated and measured pattern of the communication port is shown in Fig. 13. The maximum simulated gain is 11.2 dBi, meanwhile the measured result for communication port is 10.9 dBi, which exhibits a small decrease of 0.3 dB. The measured cross polarization of the communication port is less than  $-20$  dB. The proposed antenna array has high gain, high isolation and low cross polarization. All these advantages meet the requirements of SWIPT operation.

### C. MEASUREMENT OF THE COMMUNICATION RECTENNA ARRAY

The SWIPT capability of the communication rectenna array has been verified. The schematic of the system is shown in Fig. 1, and the experimental setup is shown in Fig. 14. The signal sources for generating CW and modulated signals are the same as those used for the rectifier measurement. A  $2 \times 4$  circular-polarized array is used as the transmitting antenna, which has the measured reflection coefficient  $|S_{11}|$  less than  $-10$  dB from 2.40 to 3.17 GHz, the axial ratio (AR) less than 3 dB from 2.50 to 3.17 GHz and the maximum gain of 17.5 dBi.

Since the communication rectenna array is located in the near-field region (1 meter away from the transmitting antenna array), the Friss transmission formula is not applicable here. The received power  $P_{c3}$  of the array has been measured experimentally. The power meter of Agilent E4416A is connected to the communication port to get  $P_{c3}$ . Due to the symmetry of the array's feeding network as shown in Fig. 10 (b), the

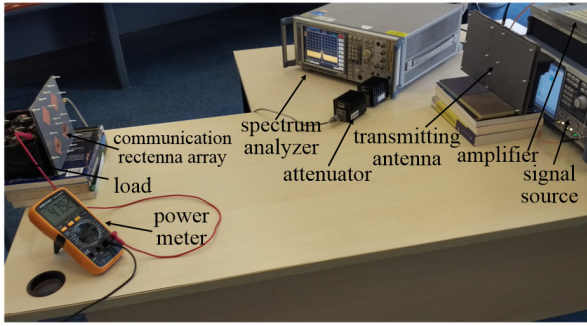


FIGURE 14. Photo of the experimental setup.

receiving power of port 2 ( $P_{r2}$ ) is the same as  $P_{c3}$ . Theoretically, the receiving power of port 1 ( $P_{r1}$ ) is 2 times of  $P_{c3}$  (i.e. plus 3 dB). However, the simulated gain difference between the rectifying port 1 and 2 is 2.6 dB. Additionally, seeing that the measured pattern of the communication port matches the simulated result, the receiving power of the rectifying port 1 ( $P_{r1}$ ) could be calculated as  $P_{r2}$  plus 2.6 dB. Therefore, the receiving power  $P_r$  for rectifying can be obtained as follows:

$$P_r = P_{r1} + P_{r2} = 2P_{r1} + 2.6(\text{dBm}) \quad (2)$$

The conversion efficiency can be calculated by the following formula,

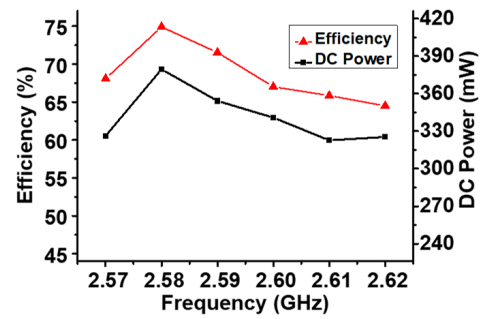
$$\eta = \frac{P_{dc1} + P_{dc2}}{P_r} = \frac{V_{dc1}^2 + V_{dc2}^2}{P_r R_L} \quad (3)$$

where  $P_{dc1/2}$  and  $V_{dc1/2}$  are the output dc power and voltage of the rectifying port 1 and 2, respectively.

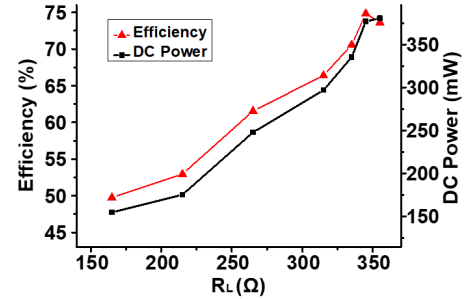
Fig. 15 shows the measured conversion efficiency of the communication rectenna array. When the input signal is CW, the conversion efficiency has a steady value of over 65 % within the band of 2.57 – 2.62 GHz with the highest value of 74.9 % at 2.58 GHz. Fig. 15 (b) shows the output voltage improves as the load increases, and the optimal load corresponding to the peak conversion efficiency is 345  $\Omega$ . The conversion efficiency varying with the input power is shown in Fig. 15 (c). The efficiency increases with the input power and reaches its maximum value of 74.9 % with the condition of an input power of 26.9 dBm and a load of 345  $\Omega$ , then the efficiency gradually decreases. The reason is that the voltage across the diode exceeds its maximum reverse voltage.

The conversion efficiency with QPSK signal is shown in Fig. 16. The peak conversion efficiency of QPSK signal is 67 % when with the signal has 10 MHz bandwidth with an input power of 26.9 dBm at 2.58 GHz carrier frequency, which is lower than that of the CW signal, but remains as an acceptable level.

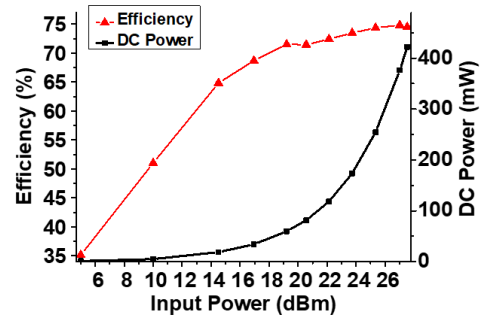
To verify the ability of communication, a signal captured from the communication port is measured using the spectrum analyzer R&S-FSQ26, as shown in Fig. 17(b). Comparing to the transmitted signal in Fig. 17(a), which is generated by the signal source, we note a relatively good agreement between the two signals, which means the proposed communication



(a)



(b)



(c)

FIGURE 15. Measured conversion efficiency and output dc power of the communication rectenna array: (a) operating frequency, (b) load, (c) input power.

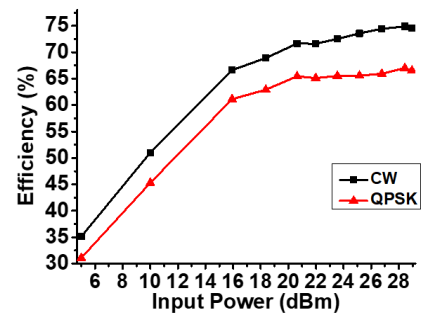
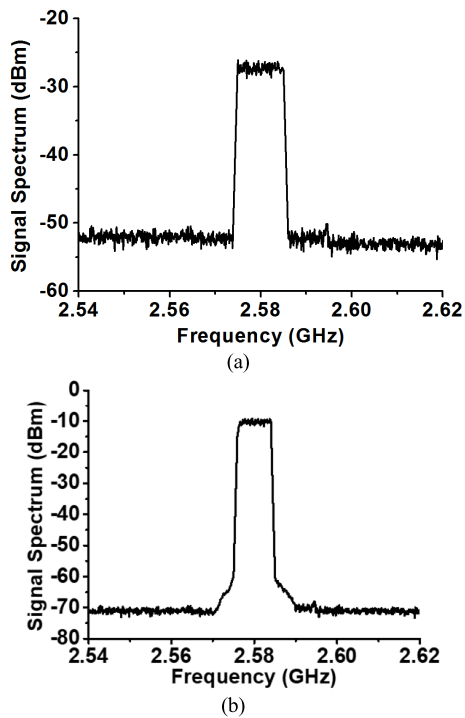


FIGURE 16. Measured efficiency of the CW and QPSK signal.

rectenna array is capable to achieve a high-quality information transmission.

The performance of some reported SWIPT systems is listed in Table 1. Compared to others' design, our work has a relatively high efficiency with a high input power of 26.9 dBm. Meanwhile, the transmission distance of our SWIPT system is one of the longest.



**FIGURE 17.** Comparison of the signal: (a) transmitted signal, (b) captured signal.

**TABLE 1.** Performance of some reported SWIPT systems.

Ref	Waveform	Frequency (MHz)	Efficiency	Distance (cm)
[19]	CW	433	86 % @ 11 dBm	50
[20]	CW	5800	64 % @ 14 dBm	80
[23]	CW	5600	50.18 % @ 5 dBm	100
[24]	multisine	6.78 ( $\Delta f = 230$ kHz)	50.7 % @ 13 dBm	1.8
[25]	pulse wave	2400	52 % @ -8 dBm	52
This work	CW	2580	74.9 % @ 26.9 dBm	100
	QPSK		67 % @ 26.9 dBm	

For a SWIPT system, the modulated waveform must be used as the transmitting waveform, which not only enables the information transmission, but also decreases the interference between the information and power transmission. Although the conversion efficiency of modulated wave is slightly lower than that of CW wave, it still remains as high as 67 % (as shown in Fig. 16), which can be considered

as high-efficient compared to existing systems. For example, in reference [23], with the same transmitting distance, the power conversion efficiency is 50.18 %. We are planning further investigation on the efficiency optimization of modulated waveform power transmission, especially for high power transmission, as well as some more realistic usages.

## VI. CONCLUSION

A novel dual-polarized communication rectenna array which allows simultaneous power and information transmission is proposed. The corner-fed  $2 \times 2$  receiving antenna array achieves high isolation and low cross polarization, so that the interference between the rectifying ports and the communication port can be minimized as much as possible. The rectifier based on the voltage doubler topology can receive high input power. The specialized feeding network could allocate more power for rectifying while meets the requirement of communication according to the difference between the sensitivity of information and power transmission. Most of the received EM signals should be used for power rectifying, and a small part for the information communication. The proposed communication rectenna array is optimized, fabricated and measured. The conversion efficiency of the communication rectenna array is measured for CW and modulated signals, respectively, and the maximum efficiency is 74.9 % for CW signal and 67 % for the QPSK signal. Meanwhile, the communication capability is verified. The measured pattern of the communication port shows that the gain is 10.9 dBi and the cross polarization is less than  $-20$  dB. The isolation between the dual-polarized ports is more than 20 dB. The proposed communication rectenna array with high power conversion efficiency and high-quality communication can be a promising candidate for the receiving part of a SWIPT system, which can be integrated into e.g. IoT, massive wireless sensor networks and biomedical implants in the future.

## REFERENCES

- [1] T. D. P. Perera, D. N. K. Jayakody, S. Chatzinotas, and J. Li, "Simultaneous wireless information and power transfer (SWIPT): Recent advances and future challenges," *IEEE Commun. Surveys Tuts.*, vol. 20, no. 1, pp. 264–302, 1st Quart., 2018.
- [2] S. Bi, Y. Zeng, and R. Zhang, "Wireless powered communication networks: An overview," *IEEE Wireless Commun.*, vol. 23, no. 2, pp. 10–18, Apr. 2016.
- [3] S.-T. Khang, J. W. Yu, and W.-S. Lee, "Compact folded dipole rectenna with RF-based energy harvesting for IoT smart sensors," *Electron. Lett.*, vol. 51, no. 12, pp. 926–928, 2015.
- [4] A. Afyf, M. A. Sennouni, L. Bellarbi, A. Achour, and N. Yaakoubi, "Enhanced RF energy harvester for power efficient Internet-of-Things wireless sensors," in *Proc. 6th Int. Conf. Multimedia Comput. Syst. (ICMCS)*, Rabat, Morocco, May 2018, pp. 1–6.
- [5] S. Jiang and S. V. Georgakopoulos, "Optimum wireless powering of sensors embedded in concrete," *IEEE Trans. Antennas Propag.*, vol. 60, no. 2, pp. 1106–1113, Feb. 2012.
- [6] S. Noguchi, M. Inamori, and Y. Sanada, "Data transmission for resonant-type wireless power transfer," in *Proc. 14th Int. Symp. Wireless Pers. Multimedia Commun. (WPMC)*, Brest, France, Oct. 2011, pp. 1–5.
- [7] W. C. Brown, "The history of power transmission by radio waves," *IEEE Trans. Microw. Theory Techn.*, vol. MTT-32, no. 9, pp. 1230–1242, Sep. 1984.
- [8] J. M. Osepchuk, "Microwave power applications," *IEEE Trans. Microw. Theory Techn.*, vol. 50, no. 3, pp. 975–985, Mar. 2002.

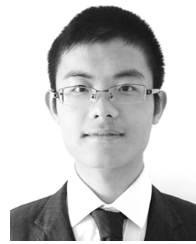


- [9] B. Strassner and K. Chang, "Microwave power transmission: Historical milestones and system components," *Proc. IEEE*, vol. 101, no. 6, pp. 1379–1396, Jun. 2013.
- [10] J. O. McSpadden and J. C. Mankins, "Space solar power programs and microwave wireless power transmission technology," *IEEE Microw. Mag.*, vol. 3, no. 4, pp. 46–57, Dec. 2002.
- [11] L. R. Varshney, "Transporting information and energy simultaneously," in *Proc. IEEE Int. Symp. Inf. Theory*, Toronto, ON, Canada, Jul. 2008, pp. 1612–1616.
- [12] L. Liu, R. Zhang, and K.-C. Chua, "Wireless information transfer with opportunistic energy harvesting," *IEEE Trans. Wireless Commun.*, vol. 12, no. 1, pp. 288–300, Jan. 2013.
- [13] O. Ozel, K. Tutuncuoglu, J. Yang, S. Ulukus, and A. Yener, "Transmission with energy harvesting nodes in fading wireless channels: Optimal policies," *IEEE J. Sel. Areas Commun.*, vol. 29, no. 8, pp. 1732–1743, Sep. 2011.
- [14] P. Grover and A. Sahai, "Shannon meets tesla: Wireless information and power transfer," in *Proc. IEEE Int. Symp. Inf. Theory*, Austin, TX, USA, Jun. 2010, pp. 2363–2367.
- [15] X. Zhou, R. Zhang, and C. K. Ho, "Wireless information and power transfer: Architecture design and rate-energy tradeoff," *IEEE Trans. Commun.*, vol. 61, no. 11, pp. 4754–4767, Nov. 2013.
- [16] A. M. Fouladgar and O. Simeone, "On the transfer of information and energy in multi-user systems," *IEEE Commun. Lett.*, vol. 16, no. 11, pp. 1733–1736, Nov. 2012.
- [17] B. Strassner and K. Chang, "Highly efficient C-band circularly polarized rectifying antenna array for wireless microwave power transmission," *IEEE Trans. Antennas Propag.*, vol. 51, no. 6, pp. 1347–1356, Jun. 2003.
- [18] H. Sun and W. Geyi, "A new rectenna with all-polarization-receiving capability for wireless power transmission," *IEEE Antennas Wireless Propag. Lett.*, vol. 15, pp. 814–817, 2016.
- [19] F.-J. Huang, C.-M. Lee, C.-L. Chang, L.-K. Chen, T.-C. Yo, and C.-H. Luo, "Rectenna application of miniaturized implantable antenna design for triple-band biotelemetry communication," *IEEE Trans. Antennas Propag.*, vol. 59, no. 7, pp. 2646–2653, Jul. 2011.
- [20] X. X. Yang, C. Jiang, A. Z. Elsherbeni, F. Yang, and Y. Q. Wang, "A novel compact printed rectenna for data communication systems," *IEEE Trans. Antennas Propag.*, vol. 61, no. 5, pp. 2532–2539, May 2013.
- [21] S. C. Gao, L. W. Li, P. Gardner, and P. S. Hall, "Dual-polarised wide-band microstrip antenna," *Electron. Lett.*, vol. 37, no. 18, pp. 1106–1107, Aug. 2001.
- [22] J. O. McSpadden, L. Fan, and K. Chang, "Design and experiments of a high-conversion-efficiency 5.8-GHz rectenna," *IEEE Trans. Microw. Theory Techn.*, vol. 46, no. 12, pp. 2053–2060, Dec. 1998.
- [23] P. Lu, X.-S. Yang, and B.-Z. Wang, "A two-channel frequency reconfigurable rectenna for microwave power transmission and data communication," *IEEE Trans. Antennas Propag.*, vol. 65, no. 12, pp. 6976–6985, Dec. 2017.
- [24] Z. Liu, Z. Zhong, and Y.-X. Guo, "In vivo high-efficiency wireless power transfer with multisine excitation," *IEEE Trans. Microw. Theory Techn.*, vol. 65, no. 9, pp. 3530–3540, Sep. 2017.
- [25] R. Ibrahim, D. Voyer, M. El Zoghbi, J. Huillery, A. Bréard, C. Vollaïre, Y. Zaatari, B. Allard, "Novel design for a rectenna to collect pulse waves at 2.4 GHz," *IEEE Trans. Microw. Theory Techn.*, vol. 66, no. 1, pp. 357–365, Jan. 2018.



**GE-LIANG ZHU** received the B.S. degree from Shanghai University, Shanghai, China, in 2017, where he is currently pursuing the M.S. degree in electromagnetic field and microwave technology.

His current research interests include microwave power transmission and rectenna.



JIN-XIN DU was born in Hebei, China, in 1989.

He received the M.S. degree in electronics from Beihang University, Beijing, China, in 2014, the Engineer degree from the Ecole Centrale de Lyon, Lyon, France, in 2014, and the Ph.D. degree in microwaves and radio-frequency from Télécom ParisTech, Paris, France, in 2018.

He has been a Lecturer at Shanghai University, since 2018. His research activities are in the areas of textile antennas, statistical quantification of disturbed antennas, and rectennas.



**XUE-XIA YANG** (M'05–SM'17) received the B.S. and M.S. degrees from Lanzhou University, Lanzhou, China, in 1991 and 1994, respectively, and the Ph.D. degree in electromagnetic field and microwave technology from Shanghai University, Shanghai, China, in 2001.

From 1994 to 1998, she was a Teaching Assistant and a Lecturer with Lanzhou University. From 2001 to 2008, she was a Lecturer and an Associate Professor with Shanghai University, where

she is currently a Professor and the Head of the Antennas and Microwave Research and Development Center. She has authored or coauthored more than 180 technical journal and conference papers. Her current research interests include antennas theory and technology and computational electromagnetics, and microwave power transmission.

Dr. Yang is currently a member of the Committee of Antenna Society of China Electronics Institute and a Senior Member of the China Electronics Institute. She is a frequent Reviewer for more than ten scientific journals. She is an Associate Editor of the *Journal of Shanghai University* (Science Edition).



**YONG-GANG ZHOU** was born in Neijiang, China, in 1972. He received the B.S., M.S., and Ph.D. degrees from the Nanjing University of Aeronautics and Astronautics, Nanjing, China, in 1993, 2000, and 2006, respectively, where he is currently an Associate Professor with the College of Electronic Information Engineering.

His research interests are in the areas of microwave circuits and components design, antenna design, and RF simulation system technology.



**STEVEN GAO** received the Ph.D. degree in microwave engineering from Shanghai University, Shanghai, China, in 1999.

He is currently a Professor and the Chair of the RF and microwave engineering with the University of Kent, Canterbury, U.K. His current research interests include smart antennas, phased arrays, MIMO, satellite antennas, satellite communications, UWB radars, synthetic aperture radars, and mobile communications.

...